

Article

# From Newspaper Substrate to Nanotubes—Analysis of Carbonized Soot Grown on Kaolin Sized Newsprint

Bruce E. Brinson <sup>1,\*</sup>, Varun Shenoy Gangoli <sup>1</sup>, Anjali Kumar <sup>2</sup>, Robert H. Hauge <sup>1,†</sup>,  
W. Wade Adams <sup>2</sup> and Andrew R. Barron <sup>1,2,3,\*</sup>

<sup>1</sup> Department of Chemistry, Rice University, Houston, TX 77005, USA; varunshenoyg@rice.edu

<sup>2</sup> Department of Materials Science and Nanoengineering, Rice University, Houston, TX 77005, USA; anjali.kumar@rice.edu (A.K.); wadams@rice.edu (W.W.A.)

<sup>3</sup> Energy Safety Research Institute, Swansea University Bay Campus, Swansea SA1 8EN, UK

\* Correspondence: brinson@rice.edu (B.E.B.); arb@rice.edu (A.R.B.); Tel.: +44-01792-606930 (A.R.B.)

† Deceased 17 March 2016.

Received: 4 October 2019; Accepted: 27 October 2019; Published: 29 October 2019



**Abstract:** Herein, we report the successful use of newspaper as a substrate for the growth of single-walled carbon nanotubes (SWCNTs) by chemical vapor deposition (CVD) with intriguing results demonstrating that (a) the large surface area of newspaper stock allows for SWCNT growth and (b) only newspaper produced with kaolin clay sizing allowed for SWCNT growth. Kaolin newsprint was impregnated with  $\text{Al}_2\text{O}_3$  and  $\text{Fe}(\text{NO}_3)_3 \cdot 9\text{H}_2\text{O}$  (as precursors to  $\text{Fe}_x\text{O}_y$  nanoparticles), and calcined (30 min at 400 °C). The subsequent char residue was loaded into a CVD chamber and used as a substrate for SWCNT growth at 750 °C, using  $\text{H}_2$ ,  $\text{C}_2\text{H}_2$ , and water vapor as the growth gas. Samples of raw carbon soot exhibiting fluorescence spectra, indicative of SWCNTs, were further evaluated by resonant Raman spectroscopy, and by transmission electron microscopy (TEM). The calcinated substrate remnants were evaluated by scanning electron microscopy (SEM) and energy dispersive X-ray spectroscopy (EDS). Experiments utilizing paper substrates produced with kaolin filler resulted in hybridized  $\text{sp}^2$ – $\text{sp}^3$  bonded carbon species. The soot was found to consist primarily of carbon nanotubes and bi-layer graphene in the form of collapsed nanotubes, also known as graphene nanoribbons (GNR).

**Keywords:** carbon; carbon nanotube; circular economy; carbon recycling; green manufacturing

## 1. Introduction

Despite the potential application of both single-walled carbon nanotubes (SWCNTs) and multi-walled carbon nanotubes (MWCNTs) for a broad range of research and commercial fields extending from electronics to medicine [1,2], their purity is of paramount importance with many of the end-uses [3]. As a result, we have, among other things, concentrated much of our research efforts in developing purification methods to remove amorphous carbon, catalyst residue and defects [4–6]. Conversely, one of the most commonly raised value enhancements of materials by CNTs is the modification of elastomer properties [7], where purity can actually be detrimental in some cases. This has led towards the use of larger MWCNTs that are inherently more defective, and hence easier to functionalize; however, there are limits on the number of concentric CNT tube walls before MWCNT embrittlement becomes an issue [8]. For polymer matrices, mixtures of graphitic carbon, CNTs, and carbon black (CB) are of interest and have been shown to improve/preferentially modify CNT dispersion, electrical conductivity, mechanical reinforcement, and surface properties [9–11]. A further consideration is that rubber compound reinforcing materials are considered as commodity products,

and thus production cost is a critical consideration. A continuous flow method by which inexpensive heterogeneous CNT/CB products can be mass-produced and applied to rubber compounding, especially one that does not require industrial retooling, would hence be quite advantageous.

CNT synthesis has been a subject of interest in research labs around the world for multiple decades, and much has been learned, especially when it comes to chemical vapor deposition (CVD) [12–15]. CVD synthesis of CNTs began with directed growth on substrates but has since evolved to include floating-catalyst growth that is substrate-free, especially as it comes to more commercial-scale production [16,17] utilizing a larger reaction volume. In addition, to process control and cost considerations, there is also a need to adopt greener and environment friendly synthesis methods utilizing natural, renewable, cheaper waste materials [18]. In this regard, the synthesis of graphene, CNTs and carbon dots has been reported using several natural hydrocarbon precursors, as well food waste, vegetation waste, animal/bird/insect waste, and agro-waste for the synthesis of graphene and CNTs [19,20]. A second component, the growth catalyst, has also been investigated using natural materials [21]; however, there are limited studies on alternative substrates.

One of the challenges here is that large scale CVD growth of carbon nanotubes from fixed substrates is hampered by the cost of substrate preparation in addition to limitations of single surface batch processing as it comes to scaling up the process. A continuous flow system, that dramatically reduces both substrate and post synthesis process cost, needs to be devised. Common substrate preparation methods combine  $\text{Fe}_x\text{O}_y$  catalyst particles with silica, silicon and alumina films [22–24]. Fixed bed CVD, the method used in this study, typically utilizes a single surface substrate. This clearly limits scalability relative to 3D or continuously formed substrates. As part of our exploration of potential stackable (3D), currently mass-produced, large-area and inexpensive substrates to produce a CNT containing soot product compatible with current industrial tooling, we investigated the use of newsprint as a substrate. Paper has been previously employed as a flexible substrate for CNT growth [21,25]; however, this was limited to relatively small areas and varying degrees of success. Herein we report that hybridized graphitic-SWCNT-carbon black soot is rapidly grown on stacks of kaolin (china clay) sized newspaper stock, which makes it suitable as part of a method capable of using a multi-surface continuous feed process.

## 2. Experimental Section

### 2.1. Materials

$\text{Al}_2\text{O}_3$  powder (>99%),  $\text{Fe}(\text{NO}_3)_3 \cdot 9\text{H}_2\text{O}$  (>98%), and ethanol (200 proof, >99.5% pure) were obtained from Sigma Aldrich (St Louis, MO, USA) and used as received, while  $\text{H}_2$  and  $\text{C}_2\text{H}_2$  were obtained from Matheson Tri-Gas Inc. (Houston, TX, USA). Newspaper samples were donated by Voice of Asia, Pasadena Citizen, and Rice Thresher (Houston, TX, USA).

### 2.2. CNT Growth

Stacks of newspaper samples ( $\sim 1.5 \times 8$  cm in area) were prepared from blank sections (containing no ink) of newsprint. The newsprint samples were dip-coated in an aqueous slurry of  $1.1 \times 10^{-3}$  wt%  $\text{Al}_2\text{O}_3$  and then immediately dipped into ethanol to promote rapid and even drying. Once dry, the samples were dip-coated in an aqueous solution of  $\text{Fe}(\text{NO}_3)_3 \cdot 9\text{H}_2\text{O}$  and again dried by dipping in ethanol. The samples were then placed into an atmospheric pressure calcination furnace (heating ramp rate of  $100\text{ }^\circ\text{C}/15\text{ min}$  to  $400\text{ }^\circ\text{C}$ , held isotherm at  $400\text{ }^\circ\text{C}$  for 30 min, and finally cooled to  $25\text{ }^\circ\text{C}$ ). After calcination, the samples were loaded into a CVD reactor, where SWCNT growth was initiated on the calcined char residue of the newspaper substrate using identical methods as previously described [26,27]. In particular, the precursor placed inside a 1-inch CVD furnace was exposed to atomic hydrogen for 30 s via the release of ultrapure  $\text{H}_2$  gas to a glowing tungsten filament. This was followed by a simultaneous flow of  $\text{H}_2$  at 0.21 standard liters per minute (SLM),  $\text{C}_2\text{H}_2$  (2.0 SLM), and water vapor (0.20 SLM) for a growth period of 5 min. The sample was then cooled to room

temperature prior to extraction for further characterization. All materials were handled in a safe manner as described previously [28].

### 2.3. Characterization

Fluorescence spectra were collected using an NS2 NanoSpectralyzer™ (Applied NanoFluorescence, LLC, Houston, TX, USA) [29]. Raman spectra were collected using a Renishaw inVia™ Raman microscope (Wotton-under-Edge, UK) equipped with 514, 633, and 785 nm lasers and a Leica PL Fluotar L50×/0.55 long working distance objective lens. Raman laser excitation powers were determined by increasing laser irradiance until the spectral transition from baseline noise to a weak signal-to-noise ratio of ~3 at ca. 1600 cm<sup>-1</sup> Raman shift was observed. The actual irradiances are unknown, and not relevant to this discussion. This resulted in a relatively flat background for the 633 and 785 nm spectra. The fluorescence background at 514 nm could not be suppressed entirely and background subtraction was performed to help better compare the three Raman spectra. Collection times were chosen to acquire >25,000 cts at ca. 1600 cm<sup>-1</sup>, and a minimum of 10 separate Raman spectrum maps were collected per sample for statistical accuracy. It is not known if or how residual support and catalyst particles affect the spectra. While generally unusual in Raman studies, for carbon species, excitation wavelength-dependent peak shifting is expected and was observed [30,31]. Carbon soot was deposited onto C-Flat™ grids (Electron Microscopy Sciences, Inc., Hatfield, PA, USA) by making physical contact at a random point in the carbon soot and imaged using a cold cathode JEOL 2100F TEM operated at 200 KV (Peabody, MA, USA). Scanning electron microscopy (SEM) energy dispersive X-ray spectra (EDS) were collected using a FEI Quanta 400 ESEM (ThermoFisher Scientific, MA, USA) equipped with an EDAX™ spectrometer (MA, USA). Elemental quantification was obtained using the ZAF (standard-less) method available in the EDAX Genesis™ application.

## 3. Results and Discussion

### 3.1. SWCNT Growth on Paper Substrates

Samples of three sources of newsprint available locally in Houston (TX) were impregnated with Fe(NO<sub>3</sub>)<sub>3</sub>·9H<sub>2</sub>O as a catalyst precursor, placed in multilayered stacks (~12 to a stack), and subjected to typical CVD conditions for the growth of SWCNTs. After growth the paper samples had the consistency of soot, which was collected together for each experiment to be further characterized. Fluorescence spectroscopy represents a useful rapid method for screening the presence of SWCNTs in a sample [32], as such fluorescence spectra were collected on all the samples; however, only the Voice of Asia sourced paper showed the presence of SWCNTs.

TEM images confirm the presence of SWCNTs with two size distributions centered at about 1 nm and 4 nm (Figure 1). Asymmetric cross-sections of the larger features confirm their tubular nature, but the irregular borders suggest these are collapsed tube structures approximating 2-layer graphene nanoribbons. Spherical structures in TEM images (Figure 1c) suggest the presence of fullerenes as well but no attempt was made to extract and identify this species.

Figure 2 shows a representative fluorescence spectrum from the experimental soot grown on the Voice of Asia newsprint, compared to that of a sample of HiPco grown SWCNTs, confirming the growth of SWCNTs. Analysis of the data suggested that the newspaper-grown sample included SWCNTs with chiralities of (7,5), (7,6), (8,3), (9,4), (9,7), (10,5), and (11,3) [32]; however, it should be noted that metallic SWCNTs are not detected in this manner, and the resolution of individual tubes versus bundles is not straightforward [3].

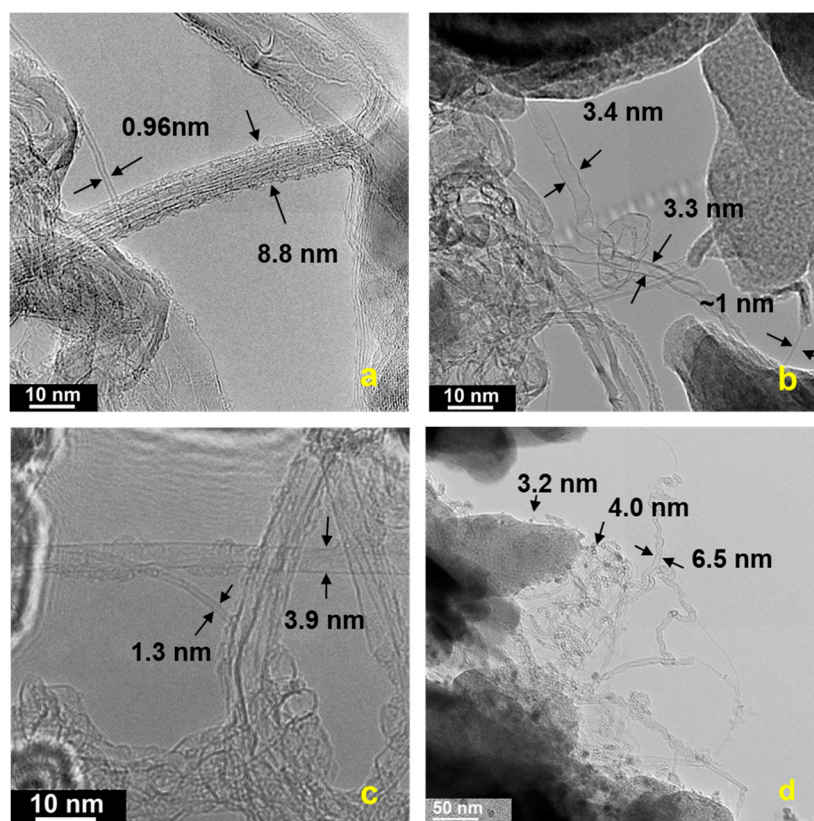


**Figure 1.** TEM images of raw carbon soot grown on kaolin sized paper showing (a) roped single-walled carbon nanotubes (SWCNTs) helically wrapped by a SWCNT, and large SWCNTs, (b) collapsed, (c) folded, and (d) twisted nanotubes. Scale bar = 10 nm (a–c) and 50 nm (d).

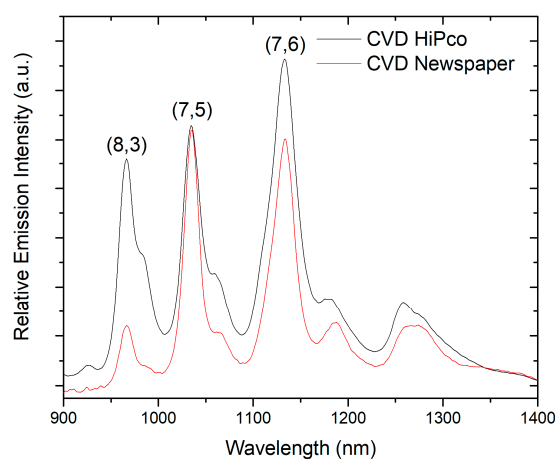


**Figure 2.** A comparison of the 660 nm excited fluorescence spectra from chemical vapor disposition (CVD) HiPco SWCNTs (black line) and CVD grown soot on “Voice of Asia” newsprint substrate (red line), depicting specific chiralities of semi-conducting SWCNTs present in both samples.

### 3.2. What Determines the Activity of a Paper Substrate for SWCNT Growth?

It was interesting that only one of the three newsprint sourced facilitated the growth of SWCNTs, despite the addition of identical quantities of catalyst precursor and process conditions. Standard newsprint is a paper grade that is mostly made out of thermo-mechanical pulp (TMP), pressure ground wood (PGW) and deinked pulp (DIP). Moreover, some softwood might be mixed in to furnish to enhance paper strengths. Sizing (filler) is used in all paper (including newsprint) to create the desired brightness level of the end product. Historically, the most common sizing agent was aluminum

sulfate (alum); however, its hydrolysis and resulting acid hydrolysis of the cellulose is a reason for the deterioration (embrittlement and yellowing) of paper in books and archival material [33,34] necessitating preservation treatments [35]. As a consequence, alkaline paper size became commercially available [36], including: Kaolin (China clay), talc, ground  $\text{CaCO}_3$  (GCC), precipitated  $\text{CaCO}_3$  (PCC), and  $\text{TiO}_2$  [37].

Energy dispersive X-ray spectroscopy (EDS) was used to analyze the elemental composition of the newsprint. Typical EDS spectra of as-is newspaper samples that facilitated SWCNT growth (Voice of Asia) and that did not facilitate SWCNT growth (Rice Thresher and Pasadena Citizen) are shown in Figure 3. The spectra of these samples prior to any carbonization are consistent with the chemical formulas of the two most common sizing agents used in newsprint: kaolin ( $\text{Al}_2\text{Si}_2\text{O}_5(\text{OH})_4$ ) and calcium carbonate ( $\text{CaCO}_3$ ) [38]. The majority of the C and O present in both samples can be attributed to the cellulose, i.e.,  $(\text{C}_6\text{H}_{10}\text{O}_5)_n$ . The “Voice of Asia” sample shows the additional presence of significant Al and Si in a 1:1 ratio (Figure 3a) in addition to minor amounts of Ca and Ti. This would suggest that this newsprint has predominantly kaolin sizing, but small quantities of  $\text{CaCO}_3$  and  $\text{TiO}_2$ . The presence of Na is likely to be due to sodium silicate that is often used for the stabilization of kaolin clay slurries [39]. In contrast, the “Rice Thresher” sample (Figure 3b) shows significant Ca content, consistent with predominantly  $\text{CaCO}_3$  sizing [40], with traces of an aluminum silicate, presumably kaolin.

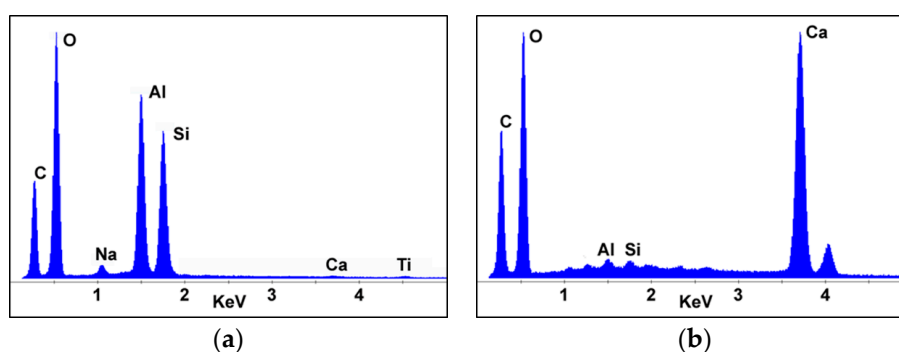


**Figure 3.** Typical energy dispersive X-ray spectroscopy (EDS) spectra of newspaper samples that facilitated SWCNT growth (a) and that did not facilitate SWCNT growth (b).

Based upon this analysis it appears that the presence of significant kaolin sizing in the newsprint was the critical factor that enabled SWCNT growth in our growth scenario. This discovery is supported by a prior report that describes the use of clay as a substrate in the growth of carbon nanotubes [41].

### 3.3. Characterization of Carbon Soot

Since the carbon soot grown by CVD on iron-impregnated kaolin sized paper was shown to contain (at least in-part) SWCNTs, a full characterization was undertaken using Raman spectroscopy. Figure 4 shows an example Raman spectra of raw carbon soot grown on kaolin sized paper, excited at 785, 633, and 514 nm, which is representative across the 10 such acquisitions collected. Table 1 lists the D, G, and 2D peak positions at each excitation wavelength. The Raman scattering cross-sections of CNTs vary with chirality, diameter, and excitation energy, with semiconducting SWCNTs the cross-sections increase with lower excitation energy. As seen in Figure 4, the NIR excited spectra (780 nm) include much more structure than do the spectra acquired with 633 and 514 nm excitation.

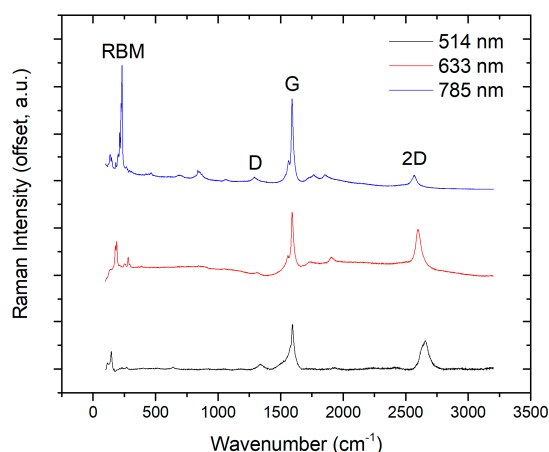


**Figure 4.** Representative normalized Raman spectra excited at (blue line) 785 nm, (red line) 633 nm, and (black line) 514 nm, of raw carbon soot grown on kaolin sized paper chosen at random. The presence of D, G, and 2D peaks confirm the presence of graphitic carbon in the form of carbon nanotubes, in addition to other forms of carbon.

**Table 1.** Resonant Raman peak intensities for the raw carbon soot grown on kaolin sized paper.

Peak	514 nm	633 nm	780 nm
D	1399	1306	1290
G	1594	1591	1591
2D	2652	2597	2566

Since the CVD synthesis temperature did not exceed 760 °C across the board, and so there is no reason to expect contribution from graphite to the Raman spectra, which would otherwise be similar to spectra from SWCNTs with a semiconducting (zigzag) structure. However, radial breathing modes, which are unique to fullerenes and single/few-walled CNTs, are present. The 2D peak shape and shift with excitation wavelength are constant with 1–2 layer graphene; however, this would be also expected to exhibit a strong D band, which is only a minor peak in the spectra in Figure 3 [30,42,43].

The well-defined G peak at ca. 1592  $\text{cm}^{-1}$  is attributed to C–C bonding and is present in all  $\text{sp}^2$  hybridized carbon species. The low energy shoulder of the G modes indicates the presence of disordered basic structural units, which can be associated with fold and twist defects exhibited by graphene nanoribbons (GNR) [8,44]. The angular changes in structure associated with GNR did not appear often in the TEM data (see above), thus, the G peak is attributed to the presence of predominantly semiconducting SWCNTs and two wall graphitic ribbons (GR) resulting from the collapse of large SWCNTs [45].

A common figure of merit (Q) for graphitic quality is the ratio of the G (graphitic) and D (disorder) modes [46]. Q can be expressed both in terms of D/G (degree of disorder) and G/D (degree of order), for the purposes of the present discussion, we assign Q to the former, i.e., a lower Q indicates few graphitic defects. Referenced to the background subtracted minima between the D and G modes, the values for  $Q_{780}$  and  $Q_{633}$  are  $\leq 0.02$ , while  $Q_{514} = 0.2$ . This variation with excitation wavelength implies a lower defect density in semiconducting structures than in the metallic species, since CNTs of average diameter 1 nm have the metallic tubes resonate at the lower excitation wavelengths of 514 and 633 nm, relative to 633 and 785 nm for semiconducting tubes [3].

The G/2D relationship allows for discerning between semiconducting and metallic SWCNT with lower values being indicative of semiconducting SWCNT [46]. The subsidiary peak on the low energy shoulder of the  $D_{780}$  and  $D_{633}$  is assigned to transverse SWCNT vibration. The strong radial breathing modes (RBM) at 780 nm, ca. 150–245  $\text{cm}^{-1}$ , are indicative of metallic SWCNT with diameters of 1 nm  $\pm$  0.05 nm while the RBMs at 514 and 633 nm suggest CNT diameters extending to 1.55 nm [43,47]. The 2D band ca. 2600  $\text{cm}^{-1}$  (also designated as  $G'$  in the literature) is common to  $\text{sp}^2$  carbon and

useful in the characterization of specific electronic and geometric structure, and doping.  $2D/G_{780} = 0.72$ , typical of semiconducting SWCNT and graphitic structure, while  $2D/G_{vis}$  is  $> 0.5$ , which is characteristic of metallic SWCNT and graphene. The unassigned bands ca.  $1700\text{ cm}^{-1}$  may be associated with  $D'$  however a  $D + D'$  band assignable to damaged graphene is not resolved ca.  $3000\text{ cm}^{-1}$  [30,48]. With  $D/G$  approaching zero in all spectra we can conclude that semiconducting SWCNT are present while the low  $G/RBM_{780}$  indicate metallic SWCNT are also present.  $G/2D_{vis} \ll G/2D_{NIR}$  is indicative of NT and/ or GR with a preferential zigzag structure.

#### 4. Conclusions

We have established that stacked kaolin filled paper is a suitable substrate for the growth of hybridized carbon soot containing semiconducting and metallic SWCNTs, and possibly bi-layer graphene ribbons with Raman characteristics of a zigzag structure, at growth temperatures that exclude the formation of graphite. The CNTs have a bimodal size distribution centered about 1 and 4 nm as seen by TEM imaging. The 4 nm tubes appear to be single walled and are clearly distorted but lack the angular features expected from fully collapsed tubes.

Capitalizing on the well-known use of alumina [22], layers of kaolin ( $\text{Al}_2\text{Si}_2\text{O}_5(\text{OH})_4$ ) filled newspaper present an attractive substrate that facilitates the reduction of iron oxide. This very likely helps in the formation of iron nanoparticles that catalyze graphitic carbon growth similar to pure alumina, while also minimizing their aggregation into larger particles which result in amorphous carbon growth instead. There remains some aggregation, however, as suggested by the formation of thicker 4 nm diameter tubes, and this allows for future improvement in product selectivity via the careful screening of more such recycled newsprint from different sources.

The use of a multi-layered substrate, such as kaolin sized newsprint, dispensed from a roll, both contained within a CVD reactor, provides for a continuous, low cost substrate, with dramatic increases in surface area relative to any ridged single surface substrate. This will lead to the reduction of greenhouse gases and exploitation of toxic materials and helps in the development of sustainable technologies as it pertains to the circular carbon economy.

**Author Contributions:** B.E.B. and A.K. performed the majority of the experiments, including the synthesis and characterization. V.S.G. helped analyze the characterization data and in writing the manuscript. R.H.H. designed the apparatus and contributed to experimental discussions. W.W.A. contributed towards discussions about the experiments and results. A.R.B. provided guidance to the experiments and helped write the manuscript. All the authors contributed to writing the manuscript.

**Funding:** This research was funded by the Office of Naval Research [N00014-15-271].

**Acknowledgments:** We acknowledge Haridayal Jaswal and Jakob Martisovits for useful discussions pertaining to this work.

**Conflicts of Interest:** The authors declare no conflict of interest.

#### References

1. Campidelli, S.; Klumpp, C.; Bianco, A.; Guldi, D.M.; Prato, M. Functionalization of CNT: Synthesis and applications in photovoltaics and biology. *J. Phys. Org. Chem.* **2006**, *19*, 531–539. [CrossRef]
2. Avouris, P.; Freitag, M.; Perebeinos, V. Carbon-nanotube photonics and optoelectronics. *Nat. Photon.* **2008**, *2*, 341–350. [CrossRef]
3. Gangoli, V.S.; Azhang, J.; Willett, T.T.; Gelwick, S.A.; Haroz, E.H.; Kono, J.; Hauge, R.H.; Wong, M.S. Using nonionic surfactants for production of semiconductor-type carbon nanotubes by gel-based affinity chromatography. *Nanomater. Nanotech.* **2014**, *4*, 19. [CrossRef]
4. Gomez, V.; Irusta, S.; Adams, W.W.; Hauge, R.H.; Durnill, C.W.; Barron, A.R. Enhanced carbon nanotubes purification by physic-chemical treatment with microwave and  $\text{Cl}_2$ . *RSC Adv.* **2016**, *6*, 11895–11902. [CrossRef]

5. Zhang, K.S.; Pham, D.; Lawal, O.; Ghosh, S.; Gangoli, V.S.; Smalley, P.; Kennedy, K.; Brinson, B.; Billups, W.E.; Hauge, R.; et al. Overcoming catalyst residue inhibition of the functionalization of single-walled carbon nanotubes via the Billups-Birch reduction. *ACS Appl. Mater. Interfaces* **2017**, *9*, 37972–37980. [[CrossRef](#)]
6. Chiang, I.W.; Brinson, B.E.; Smalley, R.E.; Margrave, J.L.; Hauge, R.H. Purification and characterization of single-wall carbon nanotubes. *J. Phys. Chem. B* **2001**, *105*, 1157–1161. [[CrossRef](#)]
7. Coleman, J.N.; Khan, U.; Blau, W.J.; Gun'ko, Y.K. Small but strong: A review of the mechanical properties of carbon nanotube–polymer composites. *Carbon* **2006**, *44*, 1624–1652. [[CrossRef](#)]
8. Pantano, A.; Parks, D.M.; Boyce, M.C. Mechanics of deformation of single- and multi-wall carbon nanotubes. *J. Mech. Phys. Solids* **2004**, *52*, 789–821. [[CrossRef](#)]
9. Carlson, T.F.; Yang, H.H.H.; Wampler, W.A. Carbon Black with Attached Carbon Nanotubes and Method of Manufacture. U.S. Patent 20080233402A1, 25 September 2008.
10. Asthana, A.; Maitra, T.; Buchel, R.; Tiwari, M.K.; Poulikakos, D. Multifunctional superhydrophobic polymer/carbon nanocomposites: Graphene, carbon nanotubes, or carbon black? *ACS Appl. Mater. Interfaces* **2014**, *6*, 8859–8867. [[CrossRef](#)]
11. Bokobza, L.; Rahmani, M.; Belin, C.; Brunell, J.-L.; Bounia, N.-E.E. Blends of carbon blacks and multiwall carbon nanotubes as reinforcing fillers for hydrocarbon rubbers. *J. Polym. Sci. B* **2008**, *46*, 1939–1951. [[CrossRef](#)]
12. Kumar, M.; Ando, Y. Chemical vapor deposition of carbon nanotubes: A review on growth mechanism and mass production. *J. Nanosci. Nanotechnol.* **2010**, *10*, 3739–3758. [[CrossRef](#)] [[PubMed](#)]
13. Tessonnier, J.-P.; Su, D.S. Recent progress on the growth mechanism of carbon nanotubes: A review. *ChemSusChem* **2011**, *4*, 824–847. [[CrossRef](#)] [[PubMed](#)]
14. Orbaek, A.W.; Barron, A.R. Towards a ‘catalyst activity map’ regarding the nucleation and growth of single walled carbon nanotubes. *J. Exp. Nanosci.* **2015**, *10*, 66–76. [[CrossRef](#)]
15. Orbaek, A.W.; Aggarwal, N.; Barron, A.R. The development of a ‘process map’ for the growth of carbon nanomaterials from ferrocene by injection CVD. *J. Mater. Chem. A* **2013**, *1*, 14122–14132. [[CrossRef](#)]
16. Bronikowski, M.J.; Willis, P.A.; Colbert, D.T.; Smith, K.A.; Smalley, R.E. Gas-phase production of carbon single-walled nanotubes from carbon monoxide via the HiPco process: A parametric study. *J. Vac. Sci. Technol. A* **2001**, *19*, 1800–1805. [[CrossRef](#)]
17. Craddock, J.D.; Weisenberger, M.C. Harvesting of large, substrate-free sheets of vertically aligned multiwall carbon nanotube arrays. *Carbon* **2015**, *81*, 839–841. [[CrossRef](#)]
18. Hedayati, A.; Barnett, C.J.; Swan, G.; White, A.O. Chemical recycling of consumer-grade black plastic into electrically conductive carbon nanotubes. *C* **2019**, *5*, 32–38. [[CrossRef](#)]
19. Kumar, R.; Singh, R.K.; Singh, D.P. Natural and waste hydrocarbon precursors for the synthesis of carbon based nanomaterials: Graphene and CNTs. *Renew. Sustain. Energy Rev.* **2016**, *58*, 976–1006. [[CrossRef](#)]
20. Deng, J.; You, Y.; Sahajwalla, V.; Joshi, R.K. Transforming waste into carbon-based nanomaterials. *Carbon* **2016**, *96*, 105–115. [[CrossRef](#)]
21. Titirici, M.-M.; White, R.J.; Brun, N.; Budarin, V.L.; Su, D.S.; del Monte, F.; Clark, J.H.; MacLachlan, M.J. Sustainable carbon materials. *Chem. Soc. Rev.* **2015**, *44*, 250–290. [[CrossRef](#)]
22. Li, Y.; Kim, W.; Zhang, Y.; Rolandi, M.; Wang, D.; Dai, H. Growth of single-walled carbon nanotubes from discrete catalytic nanoparticles of various sizes. *J. Phys. Chem. B* **2001**, *105*, 11424–11431. [[CrossRef](#)]
23. Fan, S.; Chapline, M.G.; Franklin, N.R.; Tomblor, T.W.; Cassell, A.M.; Dai, H. Self-oriented regular arrays of carbon nanotubes and their field emission properties. *Science* **1999**, *293*, 512–514. [[CrossRef](#)] [[PubMed](#)]
24. Amama, P.B.; Pint, C.L.; Kim, S.M.; McJilton, L.; Eyink, K.G.; Stach, E.A.; Hauge, R.H.; Maruyama, B. Influence of alumina type on the evolution and activity of alumina-supported Fe catalysts in single-walled carbon nanotube carpet growth. *ACS Nano* **2010**, *4*, 895–904. [[CrossRef](#)] [[PubMed](#)]
25. Glatzel, S.; Schnepf, Z.; Giordano, C. From paper to structured carbon electrodes by inkjet printing. *Angew. Chem. Int. Ed.* **2013**, *52*, 2355–2358. [[CrossRef](#)]
26. Alvarez, N.T.; Li, F.; Pint, C.L.; Mayo, J.T.; Fisher, E.Z.; Tour, J.M.; Colvin, V.L.; Hauge, R.H. Uniform large diameter carbon nanotubes in vertical arrays from premade near-monodisperse nanoparticles. *Chem. Mater.* **2011**, *23*, 3466–3475. [[CrossRef](#)]
27. Pint, C.L.; Pheasant, S.T.; Parra-Vasquez, A.N.G.; Horton, C.; Xu, Y.; Hauge, R.H. Investigation of optimal parameters for oxide-assisted growth of vertically aligned single-walled carbon nanotubes. *J. Phys. Chem. C* **2009**, *113*, 4125–4133. [[CrossRef](#)]

28. Gangoli, V.S.; Raja, P.M.V.; Esquenazi, G.L.; Barron, A.R. The safe handling of bulk low-density nanomaterials. *SN Appl. Sci.* **2019**, *1*, 644. [[CrossRef](#)]
29. Rocha, J.-D.R.; Bachilo, S.M.; Ghosh, S.; Arepalli, S.; Weisman, R.B. Efficient spectrofluorimetric analysis of single-walled carbon nanotube samples. *Anal. Chem.* **2011**, *83*, 7431–7437. [[CrossRef](#)]
30. Dresselhaus, M.S.; Jorio, A.; Hofmann, M.; Dresselhaus, G.; Saito, R. Perspectives on carbon nanotubes and graphene Raman spectroscopy. *Nano Lett.* **2010**, *10*, 751–758. [[CrossRef](#)]
31. Wang, Y.; Alsmeyer, D.C.; McCreery, R.L. Raman spectroscopy of carbon materials: Structural basis of observed spectra. *Chem. Mater.* **1990**, *2*, 557–563. [[CrossRef](#)]
32. Rao, A.M.; Richter, E.; Bandow, S.; Chase, B.; Eklund, P.C.; Williams, K.A.; Fang, S.; Subbaswamy, K.R.; Menon, M.; Thess, A.; et al. Diameter-selective raman scattering from vibrational modes in carbon nanotubes. *Science* **1997**, *275*, 187–191. [[CrossRef](#)] [[PubMed](#)]
33. Jarrell, T.D.; Hankins, J.M.; Veitch, F.P. *Deterioration of Book and Record Papers*; Technical Bulletin No. 541; US Department of Agriculture: Washington, DC, USA, 1936.
34. Barrow, W.J. *Manuscripts and Documents; Their Deterioration and Restoration*; University of Virginia Press: Charlottesville, NC, USA, 1955.
35. MacInnes, A.N.; Barron, A.R. A spectroscopic evaluation of the efficacy of two mass deacidification processes for paper. *J. Mater. Chem.* **1992**, *2*, 1049–1056. [[CrossRef](#)]
36. Schmude, K.G. Can library collections survive? The problem of paper deterioration. *Aust. Libr. J.* **1984**, *33*, 15–22. [[CrossRef](#)]
37. Bundy, W.M.; Ishley, J.N. Kaolin in paper filling and coating. *Appl. Clay Sci.* **1991**, *5*, 397–420. [[CrossRef](#)]
38. Ma, D.; Carter, R.D.; Haefner, D.; Dogariu, A. The influence of fine kaolin and ground calcium carbonates on the efficiency and distribution of fluorescence whitening agents (FWA) in paper coating. *Nord. Pulp Pap. Res. J.* **2008**, *23*, 327–332. [[CrossRef](#)]
39. Stempkowska, A.; Mastalska-Popławska, J.; Izak, P.; Ogłaza, L.; Turkowska, M. Stabilization of kaolin clay slurry with sodium silicate of different silicate moduli. *Appl. Clay Sci.* **2017**, *146*, 147–151. [[CrossRef](#)]
40. Brown, R. Physical and chemical aspects of the use of fillers in paper. In *Paper Chemistry*; Roberts, J.C., Ed.; Springer: Dordrecht, The Netherlands, 1996.
41. Gournisa, D.; Karakassidesa, M.A.; Bakasb, T.; Boukosc, N.; Petridis, D. Catalytic synthesis of carbon nanotubes on clay minerals. *Carbon* **2002**, *40*, 2641–2646. [[CrossRef](#)]
42. Ferrari, A.C.; Meyer, J.C.; Scardaci, V.; Casiraghi, C.; Lazzeri, M.; Mauri, F.; Piscanec, S.; Jiang, D.; Novoselov, K.S.; Roth, S.; et al. Raman spectrum of graphene and graphene layers. *Phys. Rev. Lett.* **2006**, *97*, 187401. [[CrossRef](#)]
43. Costa, S.; Borowiak-Palen, E.; Kruszyńska, M.; Bachmatiuk, A.; Kalenczuk, R.J. Characterization of carbon nanotubes by Raman spectroscopy. *Mater. Sci. Pol.* **2008**, *26*, 433–441.
44. Gerspacher, D.M. Carbon black characterization. In *Internal Report*; Sid Richardson Carbon Co.: Fort Worth, TX, USA, 1999.
45. Choi, D.H.; Wang, Q.; Azuma, Y.; Majima, Y.; Warner, J.H.; Miyata, Y.; Shinohara, H.; Kitaura, R. Fabrication and characterization of fully flattened carbon nanotubes: A new graphene nanoribbon analogue. *Sci. Rep.* **2013**, *3*, 1617. [[CrossRef](#)]
46. Dresselhaus, M.S.; Saito, R.; Jorio, A. Semiconducting carbon nanotubes. In Proceedings of the 27th International Conference on the Physics of Semiconductors (ICPS-27), Flagstaff, AZ, USA, 26–30 July 2004; pp. 25–31.
47. Jorio, A.; Filho, A.G.S.; Dresselhaus, G.; Dresselhaus, M.S.; Swan, A.K.; Unlu, M.S.; Goldberg, B.B.; Pimenta, M.A.; Hafner, J.H.; Lieber, C.M.; et al. G-band resonant Raman study of 62 isolated single-wall carbon nanotubes. *Phys. Rev. B* **2002**, *65*, 155412. [[CrossRef](#)]
48. Motta, M.; Moisala, A.; Kinloch, I.A.; Windle, A.H. High-performance fibres from ‘dog bone’: Carbon nanotubes. *Adv. Mater.* **2007**, *19*, 3721–3726. [[CrossRef](#)]

